Table 1. Distribution of cancer cases in a cohort of 2601 married couples, Saitama, Japan, 1986–2000

Site (ICD-9[a])	No. of couples with this cancer		
	Wives only	Husbands only	Both
Mouth and pharynx (140–149)	0	5	0
Esophagus (150)	2	10	0
Stomach (151)	32	86	2
Small intestine (152)	1	1	0
Colon (153)	7	13	1
Rectum (154)	3	12	0
Liver (155)	11	19	0
Gallbladder (156)	5	5	0
Pancreas (157)	3	17	0
Other digestive (158, 159)	0	6	0
Larynx (161)	0	9	0
Lung (162)	11	46	1
Other respiratory (163–165)	4	3	0
Melanoma (172)	2	2	0
Non-melanoma skin (173)	1	1	0
Breast (174, 175)	10	0	0
Genital organs (179–187)	16	10	0
Bladder (188)	2	11	0
Kidney (189)	1	6	0
Brain and CNS (191–192)	1	7	0
Thyroid (193)	2	1	0
Non-hodgkins lymphoma (200, 202)	1	6	0
Multiple myeloma (203)	2	1	0
Myeloid leukemia (205)	2	1	0
Other unspecified leukemia (207)	0	1	0
All cancer combined (140–209)	119	279	33
Tobacco-related (140–150, 157, 161, 162, 188)	21	102	1
Alcohol-related (140–145, 150, 155, 161)	15	98	1

[a] The International Classification of Diseases, 9th Revision.

84% for husbands and 10% for wives. Only these habits were suggested to be associated with individual cancer risk ($p < 0.1$). Husbands' smoking habits were not associated with an increased risk of cancer among 2337 non-smoking wives (adjusted RR: 0.79, 95% CI: 0.52–1.22). Mean body mass index was 22.2 for husbands and 22.6 for wives, and was not associated with individual cancer risk ($p > 0.1$). About 20% of subjects had at least one parent who had developed cancer prior to the survey, and were not at an increased risk of developing cancer (age- and birth year-adjusted RR: 1.11, 95% CI: 0.89–1.39). Thus we selected smoking and drinking habits to examine a possible relation to spousal concordance of cancer incidence.

Table 3 shows spousal concordance for all cancers in relation to shared lifestyles, using the 1872 case–control couples. Wives whose husbands developed cancer were at an increased risk of developing cancer, compared with those whose husbands had not had cancer (age- and birth year-adjusted CR: 1.70, 95% CI: 1.12–2.58). Correlation of paired cancer incidence was consistently seen, when further adjusted for smoking and drinking habits, and parental history of cancer on the baseline rates (adjusted CR: 1.74, 95% CI: 1.14–2.65). Observed correlation was more prominent among the couples whose wife's age at diagnosis was prior to the husband's age at diagnosis (adjusted CR: 1.98, 95% CI: 1.19–3.18). Particularly stronger correlation was seen among couples who shared habits of smoking or drinking. For example, the adjusted CR was 3.97 (95% CI: 1.32–11.98) for current and past smokers and 7.27 (95% CI: 1.44–36.62) for regular and past drinkers. Therefore shared smoking and drinking habits are deemed to influence spousal aggregation of cancer occurrence. The presence of spousal concordance among non-smokers (adjusted CR: 3.08, 95% CI: 1.13–8.41) may suggest the impact of further environmental factors.

Discussion

We investigated concordance of cancer incidence with lifestyle factors in a cohort of 2601 Japanese married couples in a general population, in order to establish the

Table 2. Lifestyle characteristics and cancer incidence in a cohort of 2601 married couples, Saitama, Japan, 1986–2000

	Cancer incidence			Concordance (%)		
	No. of cases	RR[a]	95% CI	Observed	Expected	*p* value[b]
Fish						
Daily	129	1[c]	–	65.4	49.4	0.02
2–4/week	274	0.81	0.66–1.00			
0–1/week	61	1.00	0.73–1.35			
Meat						
Daily	88	1[c]	–	63.0	46.9	0.02
2–4/week	288	0.98	0.77–1.24			
0–1/week	88	1.05	0.78–1.41			
Fruits						
Daily	208	1[c]	–	56.3	38.3	<0.01
2–4/week	190	0.83	0.68–1.01			
0–1/week	66	0.95	0.71–1.25			
Soy products						
Daily	167	1[c]	–	60.0	44.0	0.02
2–4/week	249	0.97	0.80–1.18			
0–1/week	48	0.95	0.69–1.31			
Eggs						
Daily	195	1[c]	–	55.8	41.0	0.02
2–4/week	215	0.98	0.81–1.19			
0–1/week	54	1.04	0.77–1.41			
Dairy products						
Daily	165	1[c]	–	48.7	33.8	0.01
2–4/week	113	0.89	0.70–1.14			
0–1/week	185	0.93	0.75–1.14			
Vegetables						
Daily	276	1[c]	–	58.6	43.5	0.02
2–4/week	141	1.01	0.82–1.24			
0–1/week	46	0.96	0.70–1.32			
Green vegetables						
Daily	167	1[c]	–	59.8	41.1	<0.01
2–4/week	227	0.97	0.79–1.19			
0–1/week	70	1.15	0.87–1.53			
Yellow vegetables						
Daily	38	1[c]	–	60.8	43.3	0.01
2–4/week	244	1.01	0.72–1.42			
0–1/week	181	1.04	0.73–1.48			
Smoking habits						
Never	167	1[c]	–	22.1	19.9	0.61
Past	75	1.45	1.03–2.05			
Current	222	1.53	1.15–2.04			
Alcohol habits						
Never	170	1[c]	–	25.8	21.4	0.34
Past	28	1.66	1.08–2.53			
Occasional	87	0.96	0.73–1.26			
Regular	179	1.22	0.94–1.58			
Body mass index						
<18.5	50	1[c]	–	60.9	59.4	0.85
18.5–25.0	345	1.00	0.74–1.36			
25.0<	66	0.89	0.61–1.30			

[a] After adjustment by Cox regression for age, sex, birth year, parental family history of cancer, and age at the time of survey.
[b] Based on the χ^2 test comparing observed and expected concordance frequency.
[c] Reference category.

Table 3. Relation of shared lifestyle with concordance of cancer incidence, in a case–control sample of 1872 married couples, Saitama, Japan, 1986–2000

	No. of couples with cancer	CR[a]	95% CI	*p* values[b]
Overall	33	1.74	1.14–2.65	
Order of diagnoses				
Wife was the first	23	1.98	1.19–3.18	0.35
Husband was the first	10	1.39	0.68–2.58	
Smoking habits				0.12
Both are current or former smokers	5	3.97	1.32–11.98	
One is a current or former smoker, and the other is a non-smoker	22	1.34	0.81–2.22	
Both are non-smokers	6	3.08	1.13–8.41	
Drinking habits				0.02
Both are regular or past drinkers	3	7.27	1.44–36.62	
One is a regular or past drinker, and the other is an occasional or non-drinker	23	2.30	1.36–3.89	
Both are occasional or non-drinkers	7	0.81	0.36–1.83	
Parental history of cancer				0.79
Both husband and wife	3	2.72	0.74–10.02	
Either husband or wife	11	1.71	0.88–3.35	
Neither husband nor wife	19	1.67	0.97–2.86	

[a] After adjustment for age, smoking and drinking habits, parental history of cancer (where appropriate).
[b] Based on the likelihood ratio test examining whether CR estimates vary in a group.

role of shared environmental factors. Study subjects were aged 40 years or older to allow latency time from the start of cohabitation. Cohort members were assumed to be a homogeneous ethnic group. Our results suggested that long cohabitation resulted in similar dietary habits, in cancer incidence of wives increasing with that of their husbands, and correlation of cancer incidence was more prominent among the couples whose wife's age at diagnosis was before the husband's age at diagnosis. Furthermore, sharing smoking and/or drinking habits increased concordance of cancer incidence among married couples, while parental history of cancer did not affect it. Thus, observed excess concordance of cancer incidence seems to be influenced more by environmental aspects than by genetic predisposition. This implication is consistent with that obtained in the latest study of twins [1]. It is unlikely that our findings were generated by a bias due to heightened medical awareness, medical attention after the spouse was diagnosed with cancer, or the quality of care that the couples have jointly received, because the present study did not include latent cancers as cancer cases.

The present study used a recently proposed statistical method to analyze correlated disease rate data between pairs [17, 20]. Bias and loss of efficiency in assessing the spousal aggregation may result from ignoring follow-up time of the spouses who were cancer-free at the end of follow-up (*i.e.*, censored subjects) and who may have developed cancer later. The present data analysis strives to avoid that by using age-adjusted CRs controlling for the effects of potential risk factors on cancer rates of both probands (husbands) and spouses (wives). Other statistical methods were also recently developed for such data [21, 22], but these approaches require complex computations. Therefore we believe that our approach facilitates analyzing correlated disease rate data in future family studies.

Regarding the matching of cases with controls, we can use either the retrospective case–control design or the nested case–control design (risk-set sampling). When we preliminarily compared the results from both designs regarding age-matching, we found that the CR estimates were consistent using the present data. Thus, we presented the results from the retrospective case–control design to illustrate the method most clearly for the readers. In addition to age, another risk factor such as birth year can be used to match cases with controls. As the present data became quite sparse when matching on age and birth year of husbands, we decided to match only on age and adjusted for the effects of birth year on the baseline cancer rates.

Spousal concordance of cancer occurrence was consistently seen in the present study, even when using the wife as proband. For 152 case wives, 760 control

wives were selected randomly from cancer-free wives, matched for age. Results of the data analysis showed that husbands whose wives developed cancer were at an increased risk of developing cancer (age- and birth year-adjusted CR: 1.81, 95% CI: 1.20–2.74). Effects of smoking and drinking habits on correlation of cancer incidence were similarly seen (details on results can be obtained from the authors). As these habits are related to dietary and other lifestyle factors in a Japanese population [23], other environmental factors may affect the concordance of cancer among married couples.

Infectious agents such as Helicobacter pylori, hepatitis B and C viruses, and Human papilloma virus are unlikely to explain the observed spousal concordance of cancer incidence for the present study. Although no information regarding such infectious agents was collected in the present study, we only observed two couples with stomach cancer. There were no couples with liver cancer or with cervical cancer/penile cancer. An excess concordance of cancer incidence among couples was still observed after excluding cancers in the stomach, liver, cervix, and penis. Thus there might be other aetiological candidates for the observed but unexplained spousal aggregation of cancer.

Nutritional factors may play an important role in the carcinogenesis process for certain sites of cancer [24, 25]. Our data, however, showed no evidence that shared dietary patterns increased spousal aggregation of cancer, since the present study collected only frequency data without amount of intake. For this reason our dietary information is insufficient to compute total energy and nutrient intakes. Instead, body mass index was used as a measure of chronic energy balance, but there was no evidence of an association with cancer risk. The shared dietary patterns in food groups may suggest that some particular food items associated with cancer risk are also commonly consumed between husbands and wives; a further study may be required.

It is possible, but unlikely, that changes in lifestyle and marital status after 1986 may have influenced the present results. There was good correspondence between married couples as regards dietary habits but little correspondence in their patterns of cigarette smoking and alcohol consumption, which is consistent with results obtained in the earlier study of lifestyle among married couples [26]. It was also reported that spouse similarities in smoking decreased and those in educational attainment increased as the duration of the relationship increased [27]. If couples became separated or divorced during follow-up, this would also decrease environmental sharing, but we have no clear measure of the degree to which this occurred. Besides cohabitation, assortative mating (the tendency for individuals to choose a marital partner with similar lifestyle) may be a plausible explanation for similarities between spouses. Thus future studies of married couples should incorporate duration of marriage, changes in lifestyle and marital status, and assortative mating into analyses.

Our study has characteristics that make it different from studies of death certificates [2], epidemiologic survey [3], hospital records [4–6], commercially-based medical care program [7], and family cancer registry [8–10]. First, unlike other studies [2–10], our study collected baseline lifestyle information from the couples themselves. Second, our study has a virtually complete follow-up of cancer incidence in a general cohort of married couples, not being limited to cancer mortality [2], parental cancer history of survey participants [3], spouses of cancer patients [4–6, 8–10] or subscribers to a medical care program [7]. Third, the couples in our study tended to have common lifestyle characteristics for a longer period than those in other studies [2, 4–10]: According to Demographic Yearbook (United Nations) and Vital Statistics of Japan (Japanese Ministry of Health, Labour and Welfare), divorce rates per 1000 population in 1995 were 1.6 for Japan, 2.5 for Sweden, and 4.5 for USA. In addition, birth years of the couples in our study were chosen to be close (mean birth-year difference: 2.3 years, SD: 3.0). And our study involved a single ethnic group, unlike most of the others, in which multiple ethnic groups were involved [2, 4–10]. Thus, differences in population assessment and demographic factors may explain why an excess spousal concordance of all cancers combined has been found in some studies including ours [3, 4, 8, 10], but not in others [7]. Although the number of couples with cancer in our study was too small to examine the aggregation of specific cancer sites, we believe that this population-based cohort study, with detailed epidemiological data for 2601 couples, will provide essential findings for the effects of common lifestyle and shared environmental factors on concordance of cancer occurrence in married couples.

Finally, our primary finding – a significant concordance of cancer risk and lifestyles among married couples – suggests the importance of controlling for shared lifestyle in developing future strategies for cancer prevention. Because lifestyles in offspring at childhood and youth tend to be similar to those of parents, shared environmental effects within a family also need to be considered. Further investigation is necessary to explore the potentially important lifestyle factors for specific cancer types in a large family-cohort study.

Acknowledgements

Supported in part by Grants-in-Aid for Cancer Research from the Ministry of Education, Science, and Culture and by a grant from the Smoking Research Foundation of Japan. The first author thanks Dr Li Hsu for helpful discussion on the statistical method.

References

1. Lichtenstein P, Holm NV, Verkasalo PK, *et al.* (2000) Environmental and heritable factors in the causation of cancer. *N Engl J Med* **343**: 78–85.
2. Chen WY, Crittenden NM, Cameron WR (1961) Site distribution of cancer deaths in husband-wife and sibling pairs. *J Natl Cancer Inst* **27**: 875–892.
3. Kato I, Tominaga S, Suzuki T (1990) Correspondence in cancer history between husbands and wives. *Jpn J Cancer Res* **81**: 584–589.
4. Manfredi OL, Gross L (1968) Cancer morbidity in married couples. *J Am Geriatr Soc* **16**: 680–685.
5. Walach N, Horn Y (1973) The incidence of cancer in married couples. [Letters] *JAMA* **226**: 201.
6. Walach N, Novikov I, Milievskaya I, *et al.* (1998) Cancer among spouses: review of 195 couples. *Cancer* **82**:180–185.
7. Friedman GD, Quesenberry CP, Jr (1999) Spousal concordance for cancer incidence. *Cancer* **86**: 2413–2419.
8. Hemminki K, Dong C, Vaittinen P (2001) Cancer risks to spouses and offspring in the family-cancer database. *Genet Epidemiol* **20**: 247–257.
9. Czene K, Lichtenstein P, Hemminki K (2002) Environmental and heritable causes of cancer among 9.6 million individuals in the Swedish family-cancer database. *Int J Cancer* **99**: 260–266.
10. Hemminki K, Jiang Y (2002) Cancer risks among long-standing spouses. *Br J Cancer* **86**: 1737–1740.
11. Houlston RS, Peto J (1996) Genetic predisposition to cancer. In: Eeles RA. *et al.* eds. *Genetics and the Common Cancers*. London, Tokyo: Chapman & Hall Medical.
12. Peto J (2001) Cancer epidemiology in the last century and the next decade. *Nature* **411**: 390–395.
13. Imai K, Suga K, Nakachi K (1997) Cancer-preventive effects of drinking green tea among a Japanese population. *Prev Med* **26**: 769–775.
14. Imai K, Matsuyama S, Miyake S, *et al.* (2000) Natural cytotoxic activity of peripheral-blood lymphocytes and cancer incidence: an 11-year follow-up study of a general population. *Lancet* **356**: 1795–1799.
15. WHO (1977) International Classification of Diseases, 9th Revision (ICD-9). Geneva: WHO.
16. Clayton DG (1978) A model for association in bivariate life tables and its application in epidemiological studies of familial tendency in chronic disease incidence. *Biometrika* **65**: 141–151.
17. Hsu L, Prentice RL, Zhao LP, *et al.* (1999) On dependence estimation using correlated failure time data from case–control family studies. *Biometrika* **86**: 743–753.
18. Therneau T, Grambsh P (2000) *Modeling Survival Data Extending the Cox Model*. New York: Springer-Verlag.
19. S-PLUS 2000 programmer's guide (1999) Seattle: MatheSoft.
20. Wei LJ, Lin DY, Weissfeld L (1989) Regression analysis of multivariate incomplete failure time data by modeling marginal distributions. *JASA* **84**: 1065–1073.
21. Nielsen GG, Gill RD, Andersen PK, *et al.* (1992) A counting process approach to maximum likelihood estimation in frailty models. *Scand J Stat* **19**: 25–43.
22. Shih JH, Louis TA (1996) Inference on the association parameter in copula models for bivariate survival data. *Biometrics* **51**: 1384–1399.
23. Kato I, Tominaga S, Matsuoka I (1987) Characteristics of lifestyle of smokers and drinkers. *Jpn J Public Health* **34**: 692–701.
24. Key TJ, Allen NE, Spencer EA, *et al.* (2002) The effect of diet on risk of cancer [review]. *Lancet* **360**: 861–868.
25. Manson MM (2003) Cancer prevention – the potential for diet to modulate molecular signaling [review]. *Trends Mol Med* **9**: 11–18.
26. Kolonel LN, Lee J (1981) Husband-wife correspondence in smoking, drinking, and dietary habits. *Am J Clin Nutr* **34**: 99–104.
27. Willemsen G, Vink JM, *et al.* (2003) Assortative mating may explain spouses' risk of same disease. *BMJ* **326**: 396.

Prediction of prognosis of estrogen receptor-positive breast cancer with combination of selected estrogen-regulated genes

Nobuyuki Yoshida,[1,4] Yoko Omoto,[1] Akio Inoue,[1,5] Hidetaka Eguchi,[6] Yasuhito Kobayashi,[2] Masafumi Kurosumi,[2] Shigehira Saji,[7] Kimito Suemasu,[3] Tomoki Okazaki,[4] Kei Nakachi,[6] Toshiro Fujita[4] and Shin-ichi Hayashi[1,8]

[1]Division of Endocrinology, Saitama Cancer Center Research Institute and [2]Department of Pathology and [3]Clinics of Breast Surgery, Saitama Cancer Center Hospital, 818 Komuro, Ina-machi, Kita-Adachi-gun, Saitama 362-0806; [4]Endocrinology, University of Tokyo Graduate School of Medicine, 7-3-1 Hongo, Bunkyo-ku, Tokyo 113-0033; [5]National Institute of Advanced Industrial Science and Technology (AIST), AIST Tsukuba Central 6, 1-1 Higashi 1-chome, Tsukuba-shi, Ibaraki 305-8566; [6]Department of Radiobiology/Molecular Epidemiology, Radiation Effects Research Foundation, 5-2 Hijiyama Park, Minami-ku, Hiroshima-shi, Hiroshima 732-0815; and [7]Department of Surgery and Breast Oncology, Tokyo Metropolitan Komagome Hospital, 3-18-22 Honkomagome, Bunkyo-ku, Tokyo 113-8677

(Received February 9, 2004/Revised April 5, 2004/2nd Revised April 7, 2004/Accepted April 8, 2004)

Estrogen receptor (ER)-positive breast cancer is a distinct subpopulation of breast cancer exhibiting a high response rate to endocrine therapy. However, not all ER-positive patients respond to the therapy, and a subgrouping of ER-positive patients based on the physiology of estrogen signaling is expected to be useful for predicting the prognosis. This study has revealed that selected estrogen-regulated genes (ERGs) are useful in identification of a poor-prognosis population among ER-positive breast cancer patients. First, the expression levels of 11 ERGs, selected based on our earlier microarray study in cultured cells, were analyzed by means of real-time reverse transcription-PCR in 14 ER-positive human breast cancer tissues. The patients were clearly divided into two groups in cluster analysis. Then, we examined the expression levels of two representative ERGs, histone deacetylase 6 (HDAC6) and insulin-like growth factor binding protein 4 (IGFBP-4), in 62 ER-positive patients with immunohistochemistry to assess the impact of ERG expression on prognosis (median follow-up 4409 days). Positive HDAC6 staining was significantly correlated with a lower disease-free survival rate. Moreover, when the expression level of HDAC6 was assessed in combination with IGFBP-4 expression in the nucleus, the poor-prognosis patients were more accurately identified. This study has identified new candidate ERGs for prediction of prognosis, and we suggest that combined assessment of the expression levels of these ERGs will contribute to the clinically useful stratification of ER-positive breast cancer patients. (Cancer Sci 2004; 95: 496–502)

Breast cancer is the leading cancer in most countries in terms of cumulative incidence rate in females. The female hormone estrogen mediates the proliferation and progression of breast cancer, and endocrine therapy, which inhibits estrogen synthesis or estrogen binding to its receptor, has been a standard therapy for estrogen receptor (ER)-positive breast cancer. Tamoxifen has served as the standard endocrine agent for postmenopausal patients for more than 25 years.[1)] While the proportional reduction in recurrence is as much as 47% in ER-positive breast cancer patients receiving adjuvant tamoxifen therapy over 5 years,[2)] a significant number of patients still relapse after the therapy. Therefore, an effective way to stratify ER-positive patients is crucial for improved choice of therapy

Many investigators have considered that expression of estrogen-regulated genes (ERGs) can provide predictive markers,[3)] because their expression may indicate the presence of a functional estrogen signaling pathway. Progesterone receptor (PgR) is one of the representative ERGs, and ER-negative and PgR-positive tumors occasionally respond to tamoxifen treatment. However, in a recent meta-analysis on adjuvant endocrine treatment,[2)] the reduction in recurrence was 23% for ER-negative and PgR-positive patients, 37% for ER-positive and PgR-positive patients, and 32% for ER-positive and PgR-negative patients, and the study concluded that it was of little additional value to measure PgR in ER-positive patients to predict the response to adjuvant tamoxifen therapy.[2)] These data indicated that although PgR expression in ER-negative patients indicated a favorable response to endocrine therapy, it was not useful for stratification of ER-positive patients in terms of response to endocrine treatment. A number of studies have been performed to find other ERGs that would serve as useful predictive or prognostic markers. However, none has been established as yet (reviewed in ref. 3).

The reason may be that the expression levels of ERGs are regulated not only by estrogen, but also by other factors, and that hampers the precise evaluation of the status of estrogen signaling in terms of the expression level of an ERG alone. This led us to hypothesize that new predictive or prognositic markers could be found from a larger body of ERGs, and the prognostic accuracy would be improved by an appropriately combined assessment of more than one ERG. This strategy would highlight the estrogen signaling pathway by minimizing the influence on the expression levels of ERGs from other signaling pathways. We have already identified more than 100 ERGs in the MCF-7 human breast cancer cell line with microarray analysis,[4)] and real-time PCR is a sufficiently quantitative method to see the expression pattern of the genes in each patient. We found that ER-positive patients could be clearly divided into two groups based on the expression pattern of 11 ERGs. Immunohistochemical (IHC) analyses showed that two of the genes could be useful in prediction of the prognosis. Furthermore, combined assessment of the two genes identified a distinct population with poor prognosis among ER-positive breast cancer patients.

Materials and Methods

Tumor samples. RNA from 26 breast cancer patients for real-time reverse transcription (RT)-PCR experiments was randomly selected from the RNA collection of the breast cancer research

[8]To whom correspondence should be addressed.
E-mail: shin@cancer-c.pref.saitama.jp

Abbreviations: ER, estrogen receptor; ERG, estrogen-regulated gene; EIA, enzyme immunoassay; H&E, hematoxylin & eosin; HDAC6, histone deacetylase 6; IGFBP-4, insulin-like growth factor binding protein 4; IGFBP-5, insulin-like growth factor binding protein 5; IHC, immunohistochemistry; LBA, ligand binding assay; NR, nuclear receptor; NRIP1, nuclear receptor interacting protein 1; PDZK1, PDZ-domain containing 1; PgR, progesterone receptor; RbBP8, retinoblastoma binding protein 8; RT, reverse transcription; SELENBP1, selenium binding protein 1; TPD52L1, tumor protein D52-like 1.

project of our research institute.[5] Tissue samples for IHC studies were from 62 consecutive primary invasive ER-positive breast cancer patients that satisfied the following criteria. They had undergone mastectomy from 1986 to 1990 at the Clinics of Breast Surgery, Saitama Cancer Center Hospital after having provided written informed consent; all patients were ER-positive in enzyme immunoassay (EIA) or ligand binding assay (LBA); the number of axillary lymph nodes with confirmed metastasis ranged from 1 to 3 pathologically; no metastasis was detected in distant organs; and treated with tamoxifen according to one of three schedules: a) 1 month in every 4 months for 5 years (42 patients), b) 1 month in every 3 months for 5 years (7 patients), or c) every day for 2 years (13 patients younger than 50). The daily dose ranged from 20 to 60 mg. Some of them were treated concurrently with oral chemotherapy (Table 1). Patients treated with i.v. chemotherapy were excluded. The modified Bloom-Richardson grading scheme[6] was adopted for histological grading. Median follow-up duration was 4409 days (range 972–5846 days). Other clinicopathological characteristics are summarized in Table 1. This project was approved by the institutional review board of Saitama Cancer Institute.

RNA preparation and RT. Total RNA of tissue samples and MCF-7 human breast cancer cell line was prepared for RT by the method of Chomczynski and Sacchi,[7] digested with RQ1 DNase (Promega, Madison, WI), purified with an RNeasy mini kit (Qiagen) and reverse-transcribed with an RNA PCR Kit (TaKaRa, Otsu) using random nanomers as primers at the time of study. To provide negative control templates for selected experiments, RT was performed with the same mixture minus reverse transcriptase.

Real-time PCR. The primer sequences are shown in Table 2. All the primer sets were designed so that the PCR products included exon-exon junctions to prevent residual genomic DNA from working as a template, except for NRIP1 and KIAA1051, since the corresponding gene to the former was intronless and the genomic sequence was not available for the latter at the time of study. Control plasmids were constructed as follows. DNA fragments for each primer set were amplified using total RNA from MCF-7 cells, purified, and cloned into pGEM-T or p-GEM-T Easy vector (Promega). The sequences of the cloned fragments were confirmed. Then the plasmids were digested with *Not*I and diluted serially to make solutions containing from 100 ng/ml to 10 fg/ml plasmid to construct standard curves. The real-time PCR was performed in duplicate using iCycler iQ (Bio-Rad Laboratories, Hercules, CA) and SYBR Green PCR Master Mix (Applied Biosystems, Warrington, UK) or a QuantiTect SYBR Green PCR Kit (Qiagen) according to the manufacturers' protocols. All the measurements were performed within the linear portion of the standard curves. For NRIP1 and KIAA1051, when the measured threshold cycle was more than the least threshold cycle for the negative control templates, the result was recorded as less than the sensitivity limit (0). The results were normalized by the expression levels of β-actin.

IHC staining. Fixation, serial sectioning, paraffin embedding, and H&E staining were performed as previously described.[8] The primary antibodies used were anti-HDAC6 rabbit polyclonal antibody H-300 (Santa Cruz Biotech, Santa Cruz, CA), and anti-IGFBP-4 goat polyclonal anitibody C-20 (Santa Cruz). The staining procedure was described elsewhere[9] except for the following. For HDAC6 staining, the sections were autoclaved at 120°C for 30 min in 10 m*M* citrate buffer for antigen retrieval, and the primary antibody was used at a 1:50 dilution and incubated at 4°C overnight, Envision solution (Dako) was applied for 45 min at room temperature, and the peroxidase activity was visualized with 3,3′-diaminobenzidine and 0.03 mol/liter hydrogen peroxide for 5 min. The procedure for IGFBP-4 staining was the same, except that the primary antibody dilution was 1:25, and the secondary antibody was polyclonal antibody labeled with biotin against goat immunoglobulin in Histofine SAB-PO(G) Kit (Nichirei, Tokyo), used according to the manufacturer's protocol, and visualized with 3,3′-diaminobenzidine and hydrogen peroxide for 15 min. In a pilot study with 5 tumor samples, we performed immunostaining in 5 patients as described above, except the primary antibody was replaced with normal serum from mouse or rabbit to provide a negative control, and confirmed that no staining was observed. We also utilized two kinds of antibodies against HDAC6 from different manufacturers (Santa-Cruz and Cell Signaling Technology, Beverly, MA) and confirmed in the same specimens that both antibodies showed the same staining pattern. The normal breast epithelium was confirmed to be stained, so the staining of the normal breast epithelium was used as a positive control in each specimen. ERα was examined immunohistochemically and evaluated in terms of the Alred score. Fifty-five patients were positive and 7 were negative. ERβ immunostaining was not performed.

IHC assessment. Immunohistochemically stained slides were evaluated blindly by N.Y. IHC scoring for HDAC6 was performed as follows. The staining intensity was classified as weak (1 point), moderate (2 points), or strong (3 points). The area of each staining intensity was estimated with a light microscopy based on 25 percentiles in a representative field. The score was calculated as the weighted average (sum of

Table 1. Patients' characteristics[1]

Patient number	62	Nodal status (clinical)		Histology	
Age		Negative	24	Invasive ductal	59
Less than 50	42	Positive	38	Special	3
50 or more	20	Stage		Histological grade	
Menopausal state		I	18	I	19
Premenopausal	38	II	40	II	21
Postmenopausal	19	III	4	III	21
Unknown	5	ER (EIA or LBA)		Unknown	1
Tumor diameter		Positive	62	Chemotherapy[2]	
Less than 2 cm	21	Negative	0	UFT	28
2 cm or more	41	PgR (EIA or LBA)		UFT+cyclophosphamide	16
		Positive	49	None	18
		Negative	11		
		Unknown	2		

1) For all the patients, the number of axillary lymph nodes confirmed pathologically to exhibit metastasis ranged from 1 to 3, and no metastasis was detected in distant organs. All the patients had undergone adjuvant tamoxifen therapy.
2) Oral chemotherapies.

point×area %). The averages of three independent measurements were calculated to the first decimal place and used for statistical analyses. The intensities of staining in the cytoplasm and nucleus were not parallel for IGFBP-4, so for IGFBP-4 IHC scoring, the nucleus and cytoplasm were evaluated separately. They were scored as integers, i.e., 0 (none or slight), 1

Table 2. Primer sequences

Gene name	Abbreviation	Primer sequence	Description
β-Actin	—	5′-GCCAACCGCGAGAAGATGA-3′ 5′-CATCACGATGCCAGTGGTA-3′	Cytoskeletal protein
Cathepsin D	—	5′-CTGAGCAGGGACCCAGATG-3′ 5′-CAGGTGGACCTGCCAGTAG-3′	Proteinase
Histone deacetylase 6	HDAC6	5′-CCTTCGCCTGTGCACAGCTT-3′ 5′-CGCACCACAGCAGCACCATT-3′	Tubulin deacetylase
Insulin-like growth factor binding protein 4	IGFBP-4	5′-ACCGCAACGGCAACTTC-3′ 5′-GTCCACACACCAGCACTT-3′	Binds to IGF
Insulin-like growth factor binding protein 5	IGFBP-5	5′-ACCGCGAGCAAGTCAAGAT-3′ 5′-CTTCACTGCTTCAGCCTTCA-3′	Binds to IGF
KIAA1051	—	5′-CCACTACCTGATGCACAACTA-3′ 5′-TGATCTTGCGTTTGGCAACCT-3′	Function unknown
Nuclear receptor interacting protein 1	NRIP1	5′-CACAGTGAGAGAGGAAGCATT-3′ 5′-CAGTTCGGTGTTTGCAAGAC-3′	Transcriptional cofactor
PDZ-domain containing 1	PDZK1	5′-CAGCCAGTTTGAAACTGTTACC-3′ 5′-CTATGTCCTTGATGATTTGACCTT-3′	Function unknown
Progesterone receptor	PgR	5′-GAGCATTGAACCAGATGTGA-3′ 5′-GTTTCGAAAACCTGGCAATGA-3′	Nuclear receptor
Retinoblastoma binding protein 8	RbBP8	5′-GGAACAGCAGAAAGTCCTTCA-3′ 5′-CAGTTACTGCACAGCGATCA-3′	Binds to tumor suppressor Rb
Selenium binding protein 1	SELENBP1	5′-CAGTATTGCCAGGTCATCCA-3′ 5′-CCCACGTCCACCACATAGA-3′	Binds to selenium
Tumor protein D52-like 1	TPD52L1	5′-CAGACTACCACTGCCTACAA-3′ 5′-GGCGAATGGAGTAACTCATG-3′	Function unknown

Table 3. Classification of representative estrogen-regulated genes[1)]

Classification	Up-regulated	Down-regulated
Growth-related genes	**IGFBP-4** Cyclin A CDC6 homologue	**IGFBP-5** Quiescin Q6
Cancer-related genes	Trefoil factor 1 **RbBP8** **TPD52L1**	MYC promoter binding 1
Transcription-related genes	**PgR** **NRIP1** **HDAC6[2)]** Early growth response 3	Estrogen receptor α
Enzyme	**Cathepsin D** Asparagine synthetase Glycyl-tRNA synthase	Enolase 3 Isocitrate dehydrogenase 2 Fucosyltransferase 8
Others	**PDZK1** **KIAA1051** Stanniocalcin 2	**SELENBP1** Catenin δ2 Cadherin 8

1) Representative ERGs that showed reproducible induction with customized microarrays are shown. **Bold** indicates the genes examined in the real-time RT-PCR study. For abbreviations, see Table 2.
2) Recently shown to be tubulin deacetylase.

(weak), 2 (moderate), or 3 (strong), in a representative field, unlike the method adopted for HDAC6.

Statistical analysis. Cluster analyses for real-time PCR data were mean-centered complete linkage clustering performed with the CLUSTER program and visualized with TREEVIEW.[10] Kaplan-Meier analyses, log-rank tests, and univariate and multivariate analyses using the Cox proportional hazards model were performed with StatView software (SAS Institute, Cary, NC).

Results

Cluster analysis of ERG expression levels and patient groups in ER-positive breast cancer patients. To determine if the ER-positive breast cancer patients could be subgrouped clearly by ERG expression patterns, we examined the expression levels of 11 ERGs selected from those ERGs identified in the previous microarray study[4] in 14 ER-positive breast cancer tissues. The choice of ERGs can be arbitrary in this step, and we chose those that we thought might be important for breast cancer physiology (Table 3), considering the potential connection to molecular studies. The 11 selected genes were cathepsin D, histone deacetylase 6 (HDAC6), insulin-like growth factor binding protein 4 (IGFBP-4), insulin-like growth factor binding protein 5 (IGFBP-5), KIAA1051, nuclear receptor interacting protein 1 (NRIP1), PDZ-domain containing 1 (PDZK1), progesterone receptor (PgR), retinoblastoma binding protein 8 (RbBP8), selenium binding protein 1 (SELENBP1), and tumor protein D52-like 1 (TPD52L1). The expression levels of ERGs were examined with real-time RT-PCR, and the results were analyzed by means of cluster analysis by mean centering, complete linkage clustering. The outcomes of cluster analysis were visualized with the TREEVIEW program as shown in Fig. 1. This hierarchical clustering produced two distinct groups in ER-positive patients, i.e., in the left cluster, HDAC6 and IGFBP-4 were expressed more and IGFBP-5 and RbBP8 less than in the patients of the right cluster. This finding suggested the presence of two populations in terms of estrogen signaling, although both are regarded as simply ER-positive tumors in current clinical practice.

Since we expected that the response to endocrine manipulation might be different between these two groups, we examined a larger clinical sample for which prognostic data were available.

IHC analyses of two representative ERGs: HDAC6 and IGFBP-4. Next, we analyzed the expression levels of HDAC6 and IGFBP-4 with IHC, which we thought, based on current knowledge, may have important implications for the estrogen signaling pathway, and examined their relationship with the prognosis.

HDAC6 staining was observed in normal and malignant mammary epithelial cells. The staining was generally strong in the cytoplasm of cancer cells, and in the nuclei of normal mammary epithelial cells (Fig. 2A). The staining was very weak, if detectable, in fibroblasts and was not observed in lymphocytes or vascular endothelial cells. The IHC score of 62 cancer tissues ranged from 1.0 to 3.0 (median 1.67). To examine the effect of the expression level of HDAC6 on disease-free survival, we assessed survival curves using the Kaplan-Meier method, and identified a score of 2.2 as a clinically meaningful cut-off point for defining HDAC6 positivity (data not shown). According to the criteria, 26% of cases (16 patients) were considered as positive and 74% (46 patients) negative. There was no significant correlation with other clinicopathological factors (data not shown). Representative staining of IGFBP-4 is shown in Fig. 2B. IGFBP-4 staining was observed in almost all cell types including normal and malignant mammary epithelial cells, infiltrating cells, and vascular endothelial cells. The nucleus was the predominant locus of staining in normal mammary epithelial cells, while cytoplasm tended to stain equally or more than the nucleus in cancer cells. Cytoplasmic and nuclear staining intensities were evaluated separately because the staining was detected in both cytoplasm and nucleus and the staining intensities were not parallel. The IHC scores for the nuclei were 0 for 24% (15 patients), 1 for 47% (29 patients), 2 for 24% (15 patients), and 3 for 5% (3 patients). The IHC scores for the cytoplasm were 1 for 65% (40 patients), 2 for 32% (20 patients), and 3 for 3% (2 patients). We examined the disease-free survival curves using the Kaplan-Meier method and identified a nuclear score between 0 and 1 as a clinically meaningful cut-off point (data not shown). Seventy-six percent (47 patients) were nuclear-IGFBP-4-positive and 24% (15 patients) were negative. There was no correlation with other clinicopathological factors (data not shown). Cytoplasmic staining did not have a significant impact on the disease-free survival rate (data not shown).

Impact of ERG expression levels on prognosis. As described above, survival analyses with the expression levels of ERGs were performed on 62 patients. The disease-free survival rates

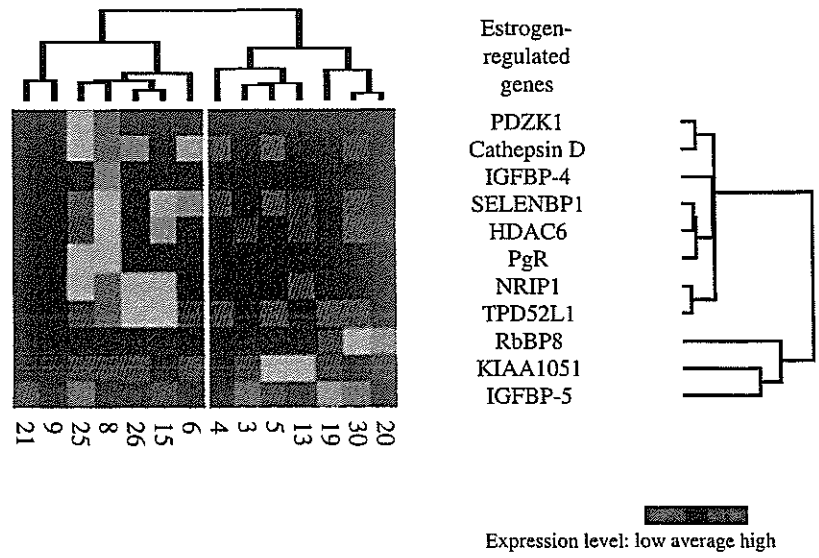

Fig. 1. Cluster analyses of the expression levels of ERGs. The expression levels of 11 ERGs were measured in 14 ER-positive breast cancer tissues and analyzed by means of cluster analysis. Numbers in the horizontal axis indicate patient numbers. On the vertical axis are ERG names. Abbreviations are the same as those in Table 1.

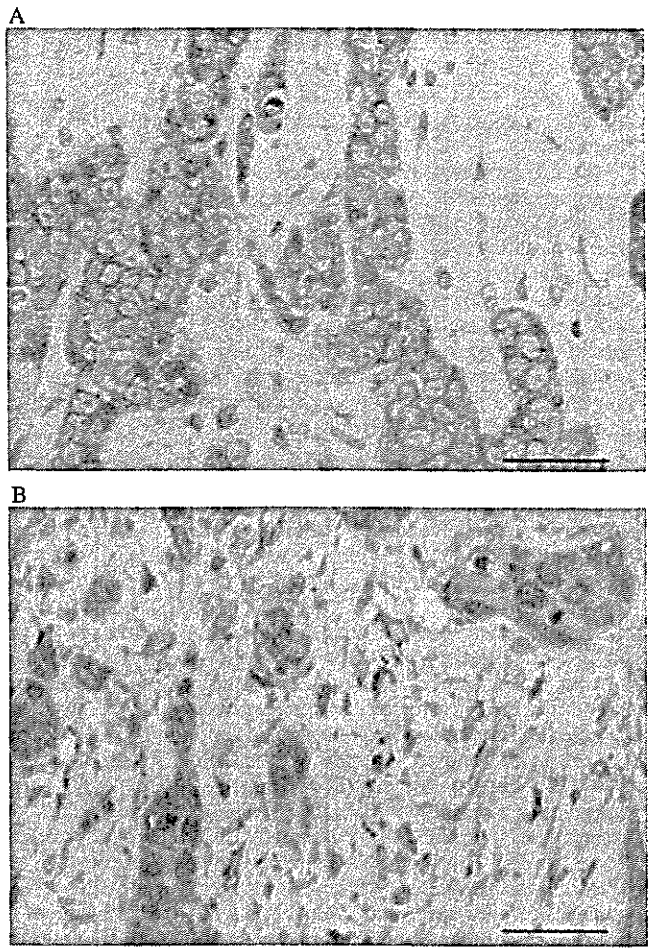

Fig. 2. Representative immunohistochemical stainings of HDAC6 and IGFBP-4 in human breast cancer tissues. A, Staining with anti-HDAC6 antibody (H-300, Santa Cruz). Staining was observed in normal and malignant mammary epithelial cells. The staining was generally strong in the cytoplasm of cancer cells, and in the nuclei of normal mammary epithelial cells. This case was scored 2.9. B, Staining with anti-IGFBP-4 antibody (C-20, Santa Cruz) showed that IGFBP-4 protein exists in both the nucleus and the cytoplasm of cancer cells. IGFBP-4 staining was observed in almost all cell types including normal and malignant mammary epithelial cells, infiltrating cells, and vascular endothelial cells. The nucleus was the predominant locus of staining in normal mammary epithelial cells, while cytoplasm tended to stain equally or more than the nucleus in cancer cells. Cytoplasmic and nuclear staining intensities were evaluated separately because the staining was detected in both cytoplasm and nucleus and the staining intensities were not parallel (the scores were 2 in the nucleus and 2 in the cytoplasm in this case). Bar: 10 μm.

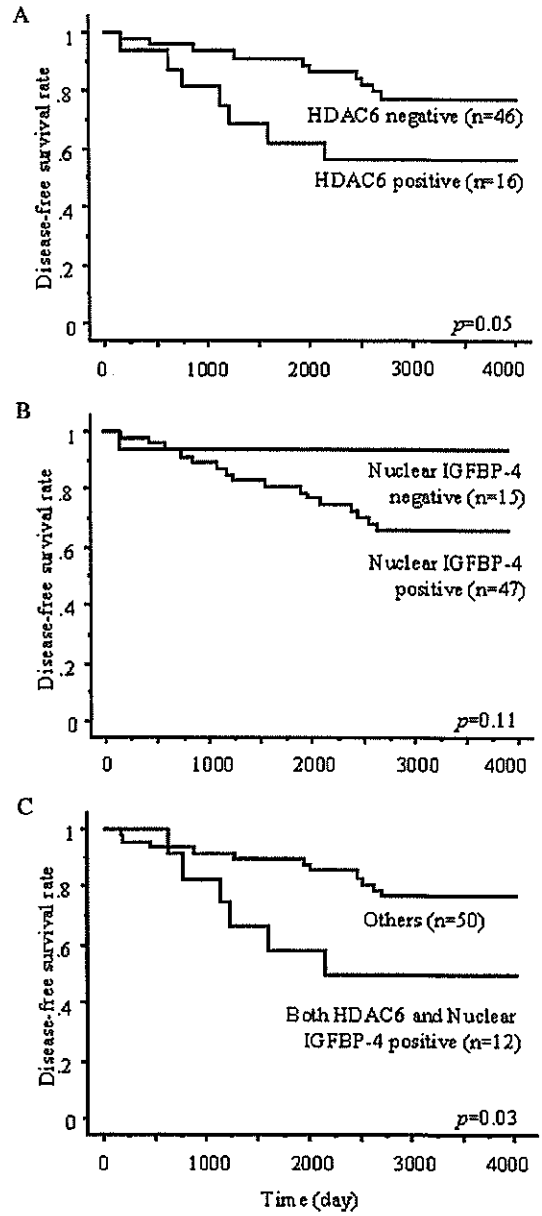

Fig. 3. Kaplan-Meier analyses of disease-free survival (DFS) and ERG expression status. A, DFS and HDAC6 status. B, DFS and nuclear IGFBP-4 status. C, DFS and combination of two ERGs, HDAC6 and IGFBP-4 (HDAC6 and IGFBP-4 double-positive cases versus others). D, DFS and combination of three ERGs, HDAC6, IGFBP-4, and PgR (HDAC6-positive, IGFBP-4-positive, and PgR-poor cases versus others). The patient subgroup unresponsive to adjuvant endocrine therapy was more accurately identified as the number of ERGs was increased. *P*: log-rank test.

for HDAC6-negative cases were significantly better than for the positive cases (Kaplan-Meier analysis $P=0.05$, Fig. 3A), although multivariate analysis (Cox proportional hazard model) showed it was not a significant prognostic factor in this study group. Positive nuclear staining for IGFBP-4 showed a trend for poor disease-free survival (Fig. 3B, not significant). Other factors including age, menopausal state, tumor diameter, stage, histology, and chemotherapy were not significant factors for disease-free survival rate. Similar trends were also seen for overall survival rates (not significant).

Finally, we tried to see if the combined assessment of the expression levels of HDAC6 and IGFBP-4 was useful to predict the prognosis.

The poor prognosis patient group was more accurately identified when the expression levels of HDAC6 and nuclear IGFBP-4 were assessed in combination, as indicated by the lower *P* value in Kaplan-Meier analysis (Fig. 3C, $P=0.03$). The disease-free survival rates at 5 years were 62.5% for HDAC6-positive cases and 78.7% for nuclear IGFBP-4-positive cases, and the rate was 58.3% when the expression levels of the two ERGs were assessed in combination. The patient group with a favorable prognosis was also identified. The 11 cases negative for both HDAC6 and nuclear IGFBP-4 showed 100% disease-free survival at 5 years. Thus, the combined assessment of the ERG expression levels improved the prognostic accuracy.

Discussion

This study showed that a newly identified ERG, HDAC6, could serve as a prognositic factor and that an appropriate combination of ERGs led to improved accuracy over one ERG alone in the detection of the poor-prognosis patient group.

The real-time RT-PCR study was intended to test the possibility of clear subgrouping of ER-positive patients. As a result, ER-positive patients were clearly classified into two groups based on the expression patterns of eleven ERGs. These 11 ERGs did not show the same expression patterns. This fact suggested that the mode of expressional regulation is not the same for all the ERGs. More comprehensive molecular and clinical studies may unravel the mechanisms involved, and our customized microarray for analyzing ERGs could be a useful tool.[4]

Next, we performed IHC analyses of selected ERGs to observe the expression patterns of ERGs, and found that the combination of HDAC6 and nuclear IGFBP-4 staining could be prognostic. The result obtained here shows the impact of these factors on the prognosis of ER-positive breast cancer patients who did not have sufficient endocrine treatment as adjuvant therapy. The current guideline on adjuvant endocrine therapy recommends administration of 20 mg/day of tamoxifen for 5 years (36 g in total) for postmenopausal women. However, the dosage was 13.5 g or 18 g in most patients enrolled for this study. Some younger patients were treated with tamoxifen every day for 2 years, but this should also be considered insufficient because surgical or medical ovariectomy is now recommended for premenopausal patients with node-positive disease, i.e., the intensity of endocrine therapy was insufficient in all the patients in the light of current knowledge.

HDAC6 expression has been reported in several tissues including the testis, liver, and brain[11, 12] and we found that it was also expressed in benign and malignant breast epithelium. Our data suggested that patients with HDAC6-positive tumors showed a poor prognosis. When HDAC6 was compared to PgR as a clinical marker, PgR was positive in 60–70% of the ER-positive patients, whereas roughly 70% of patients were HDAC6-negative in this study. Additionally, HDAC6 expression correlated with poor prognosis, while PgR expression is correlated with favorable prognosis. Although the reason for this phenomenon is unknown, it suggests that genes downstream of estrogen signaling pathway may not be regulated uniformly. Recently Hubbert *et al.* have reported that HDAC6 is a tubulin deacetylase that is targeted by taxanes, potent anticancer agents used for the treatment of breast cancer.[13] ER status has been reported not to be predictive for taxane therapy.[14] However, combination therapy of taxanes and endocrine agents may be an interesting approach for ER-positive patients with high HDAC6 expression, because taxanes counteract HDAC6 function.[13] Nuclear IGFBP-4 staining can also be a prognostic factor. A relationship between the IGFBP-4 level in culture media and tamoxifen resistance has already been reported,[15] but no report was found concerning IGFBP-4 in the nucleus and the effect of tamoxifen. It is well known that the IGFBP-4 expression is induced by estrogen, and these facts may suggest the possibility that IGFBP-4 plays a role in nuclei to stimulate growth of ER-positive breast cancer cells. Although IGFBP-4 has not been reported to function in the nucleus, IGFBP-2, IGFBP-3, and IGFBP-5 are localized at the nucleus and interact with retinoid X receptor α,[16] four and a half LIM protein 2,[17] etc. Further research on the molecular function of IGFBP-4 in the nucleus may elucidate the link between its molecular function and ER.

Moreover, a combined assessment of ERGs identified a poor-prognosis patient group more accurately than a single ERG. As already mentioned, finding subgroups among ER-positive patients can have a significant implication in the choice of therapy. Recently, many studies have tried to classify breast cancer patients according to gene expression patterns[18–23] or to predict ER status from gene expression patterns.[24, 25] However, no stratification of ER-positive patients has been reported with implications for prognosis. Our study made good use of microarray analyses that provided and characterized a large body of ERGs and real-time RT-PCR experiments that were capable of measuring the expression levels. This combinatorial study design revealed a more comprehensive picture of estrogen signaling status in cancer tissues than could be obtained with conventional studies on one ERG. Previous reports usually identified one ERG such as PgR, pS2, cathepsin D, etc. as an indicator for the signaling intensity of estrogen. However, many signaling pathways are active in cancer tissues, forming a complex signaling network. A gene generally has more than one response element or regulatory sequence in its promoter, and it is most unlikely for a gene to be regulated solely by estrogen. Now, with the development of new methodologies, combined assessment of many factors is already a practical approach and can be better than using a single indicator gene to evaluate a signaling pathway. Actually, many researchers are trying to introduce microarray analysis into clinical use. We are also developing a customized microarray technique focused on the estrogen signaling pathway for clinical use.[4] Despite much effort, microarray analysis is not immediately applicable to clinical use because it is still expensive and RNA preparation for microarray analysis as routine clinical work is only possible in a limited number of institutions. Our results suggest that combined assessment of ERG expression levels by IHC showed a performance that may be comparable to that of microarray analysis.

The most interesting problem to be coped with next is the difference in the effect of endocrine agents between the patient groups detected in this study. Other future tasks include confirmation of the observations in a larger patient group, increasing the sophistication of the IHC evaluation method by analysis of interobserver differences and other methods, and an explanation of the observations by *in vitro* studies.

To summarize, combined assessment of the expression levels of ERGs selected through microarray analyses and real-time PCR studies identified distinct prognostic subgroups among ER-positive breast cancer patients.

We thank Drs. Takako Sakamoto, Shunji Takahashi, and Yuji Tanaka for their valuable discussions, and Dr. Etsuro Ogata for his advice. We also thank Ms. Atsuko Kawarai and Ms. Akiyo Yamashita for their excellent technical assistance. This work was supported in part by Grants-in-Aid for Scientific Research from the Ministry of Education, Culture, Sports, Science and Technology of Japan, and Scientific Research Expenses for Health and Welfare Programs from the Ministry of Health, Labour and Welfare, as well as a grant from the Foundation for the Promotion of Cancer Research, and funds for the 2nd Term Comprehensive 10-Year Strategy for Cancer Control.

1. Baum M. A vision for the future? *Br J Cancer* 2001; **85** (Suppl 2): 15–8.
2. Early Breast Cancer Trialists' Collaborative Group. Tamoxifen for early breast cancer: an overview of the randomized trials. *Lancet* 1998; **351**: 1451–67.
3. Ciocca DR, Elledge R. Molecular markers for predicting response to tamoxifen in breast cancer patients. *Endocrine* 2000; **13**: 1–10.
4. Inoue A, Yoshida N, Omoto Y, Oguchi S, Yamori T, Kiyama R, Hayashi S. Development of cDNA microarray for expression profiling of estrogen-responsive genes. *J Mol Endocrinol* 2002; **29**: 175–92.
5. Hayashi S, Tanimoto K, Hajiro-Nakanishi K, Tsuchiya E, Kurosumi M, Higashi Y, Imai K, Suga K, Nakachi K. Abnormal FHIT transcripts in human breast carcinomas: a clinicopathological and epidemiological analysis

of 61 Japanese cases. *Cancer Res* 1997; **57**: 1981–5.
6. Dalton LW, Page DL, Dupont WD. Histologic grading of breast carcinoma. *Cancer* 1994; **73**: 2765–70.
7. Chomczynski P, Sacchi N. Single-step method of RNA isolation by acid guanidium thiocyanate-phenol-chloroform extraction. *Anal Biochem* 1987; **162**: 156–9.
8. Kurosumi M, Suemasu K, Tabei T, Kuwashima Y, Takeo T, Kusawake T, Higashi Y. Relationship between grade of intraductal component of breast cancer within main tumor and extent of intraductal spread in surrounding tissue. *Anticancer Res* 1998; **18**: 2869–74.
9. Omoto Y, Kobayashi Y, Nishida K, Tsuchiya E, Eguchi H, Nakagawa K, Ishikawa Y, Yamori T, Iwase H, Fujii Y, Warner M, Gustafsson J-Å, Hayashi S. Expression, function, and clinical implications of the estrogen receptor β in human lung cancers. *Biochem. Biophys. Res. Commun* 2001; **285**: 340–7.
10. Eisen MB, Spellman PT, Brown PO, Botstein D. Cluster analysis and display of genome-wide expression patterns. *Proc Natl Acad Sci USA* 1998; **95**: 14863–8.
11. Grozinger CM, Hassig CA, Schreiber SL. Three proteins define a class of human histone deacetylases related to yeast Hda1p. *Proc Natl Acad Sci USA* 1999; **96**: 4868–73.
12. Verdel A, Khochbin S. Identification of a new family of higher eukaryotic histone deacetylases. *J Biol Chem* 1999; **274**: 2440–5.
13. Hubbert C, Guardiola A, Shao R, Kawaguchi Y, Ito A, Nixon A, Yoshida M, Wang XF, Yao TP. HDAC6 is a microtubule-associated deacetylase. *Nature* 2002; **417**: 455–8.
14. van Poznak C, Tan L, Panageas KS, Arroyo CD, Hudis C, Norton L, Seidman AD. Assessment of molecular markers of clinical sensitivity to single-agent taxane therapy for metastatic breast cancer. *J Clin Oncol* 2002; **9**: 2319–26.
15. Maxwell P, van den Berg HW. Changes in the secretion of insulin-like growth factor binding proteins-2 and -4 associated with the development of tamoxifen resistance and estrogen independence in human breast cancer cell lines. *Cancer Lett* 1999; **139**: 121–7.
16. Liu B, Lee HY, Weinzimer SA, Powell DR, Clifford JL, Kurie JM, Cohen P. Direct functional interactions between insulin-like grouth factor-binding protein-3 and retinoid X receptor-alpha regulate transcriptional signaling and apoptosis. *J Biol Chem* 2000; **275**: 33607–13.
17. Amaar YG, Thompson GR, Linkhart TA, Chen ST, Baylink DJ, Mohan S. Insulin-like growth factor-binding protein 5 (IGFBP-5) interacts with a four and a half LIM protein 2 (FHL2). *J Biol Chem* 2002; **277**: 12053–60.
18. Welcsh PL, Lee MK, Gonzalez-Hernandez RM, Black DJ, Mahadevappa M, Swixher EM, Warrington JA, King M. BRCA1 transcriptionally regulates genes involved in breast tumorigenesis. *Proc Natl Acad Sci USA* 2002; **99**: 7560–5.
19. Perou CM, Sorlie T, Eisen MB, van de Rijn M, Jeffrey SS, Rees CA, Pollack JR, Ross DT, Johnsen H, Akslen LA, Fluge O, Pergamenschikov A, Williams C, Zhu SX, Lonning PE, Borresen-Dale AL, Brown PO, Botstein D. Molecular portraits of human breast tumours. *Nature* 2000; **406**: 747–52.
20. Martin KJ, Kritzman BM, Price LM, Koh B, Kwan C-P, Zhang X, Mackay A, O'Hare MJ, Kaelin CM, Mutter GL, Pardee AB, Sager R. Linking gene expression patterns to therapeutic groups in breast cancer. *Cancer Res* 2000; **60**: 2232–8.
21. Sorlie T, Perou CM, Tibshirani R, Aas T, Geisler S, Johnsen H, Hastie T, Eisen MB, van de Rijn M, Jeffrey SS, Thorsen T, Quist H, Matese JC, Brown PO, Botstein D, Lonning PE, Borresen-Dale AL. Gene expression patterns of breast carcinomas distinguish tumor subclasses with clinical implications. *Proc Natl Acad Sci USA* 2001; **98**: 10869–74.
22. Bertucci F, Houlgatte R, Benziane A, Granjeaud S, Adelaide J, Tagett R, Loriod B, Jacquemier J, Viens P, Jordan B, Birnbaum D, Nguyen C. Gene expression profiling of primary breast carcinomas using arrays of candidate genes. *Hum Mol Genet* 2000; **9**: 2981–91.
23. van't Veer LJ, Dai H, van de Vijver MJ, He YD, Hart AAM, Mao M, Peterse HL, van der Kooy K, Marton MJ, Witteveen AT, Schreiber GJ, Kerkhoven RJ, Rovberts C, Linsley PS, Bernards R, Friend SH. Gene expression profiling predicts clinical outcome of breast cancer. *Nature* 2002; **415**: 530–5.
24. West M, Blanchette C, Dressman H, Huang E, Ishida S, Spang R, Zuzan H, Olson JA Jr, Marks JR, Nevins JR. Predicting the clinical status of human breast cancer by using gene expression profiles. *Proc Natl Acad Sci USA* 2001; **98**: 11462–7.
25. Gruvberger S, Ringner M, Chen Y, Panavally S, Saal LH, Borg A, Ferno M, Peterson C, Meltzer PS. Estrogen receptor status in breast cancer is associated with remarkably distinct gene expression patterns. *Cancer Res* 2001; **61**: 5979–84.

DIABETES/METABOLISM RESEARCH AND REVIEWS
Diabetes Metab Res Rev 2004; **20**: 399–404.
Published online 22 March 2004 in Wiley InterScience (www.interscience.wiley.com). DOI: 10.1002/dmrr.469

RESEARCH ARTICLE

Increasing of oxidative stress from mitochondria in type 2 diabetic patients

Shuhei Nakanishi[1,2]*
Gen Suzuki[1]
Yoichiro Kusunoki[3]
Kiminori Yamane[2]
Genshi Egusa[2]
Nobuoki Kohno[2]

[1]*Department of Clinical Studies, Radiation Effects Research Foundation, Hiroshima, Japan*

[2]*Department of Molecular and Internal Medicine, Graduate School of Biomedical Sciences, Hiroshima University, Hiroshima, Japan*

[3]*Department of Radiobiology and Molecular Epidemiology, Radiation Effects Research Foundation, Hiroshima, Japan*

*Correspondence to:
Dr Shuhei Nakanishi, Hiroshima University-Graduate school of Biomedical Sciences, Radiation Effects Research Foundation, Department of Molecular and Internal Medicine, 5-2 Hijiyama Park, Minami-ku, Hiroshima, 732-0815, Japan. E-mail: nshuhei@rerf.or.jp

Received: 17 November 2003
Revised: 22 January 2004
Accepted: 26 January 2004

Abstract

Background Recent evidence increasingly indicates that oxidative stress may play an important role in the pathogenesis of diabetic vascular complications. Mitochondria has received much attention as an important organ in the generation of oxidative stress. However, the importance of oxidative stress among diabetic patients without vascular complications is unclear.

Methods We compared oxidative stress produced from mitochondria of the mononuclear cells in peripheral blood obtained from 26 diabetic subjects without clinical vascular complications and 52 healthy age-matched subjects using a flow cytometer. Oxidative stress from the mononuclear cells was evaluated by measuring fluorescence of oxidized production from dihydrorhodamine-123, which is a pro-fluorescent compound that selectively accumulates in the mitochondria of living cells. Stimulation of the cells was carried out with phorbol 12-myristate 13-acetate (PMA), a protein kinase C (PKC) activator. We then calculated the relative fluorescence variation (RFV) that indicated an increasing rate of oxidative stress levels by stimulation with PMA against the levels obtained at baseline. Additionally, we measured the urinary stress markers, 8-hydroxydeoxyguanosine (8OHdG) and 8-epi-prostaglandin F2α (isoprostane).

Results Compared to healthy subjects, diabetic subjects did not exhibit significantly elevated oxidative stress levels at baseline, but did have significantly elevated basal urinary 8OHdG, urinary isoprostane and oxidative stress levels after PMA stimulation as well as RFV.

Conclusions Among diabetic subjects without clinical vascular complications, there was a possibility that mitochondrial oxidative stress balance between generation and scavenging against the additive PKC stimulation was thought to have already been lost. Copyright © 2004 John Wiley & Sons, Ltd.

Keywords oxidative stress; mitochondria; type 2 diabetes mellitus; flow cytometry

Introduction

The relationship between oxidative stress and many diseases has recently received considerable attention. Under a chronic hyperglycemic state, tricarboxylic acid cycle activation in the mitochondria is thought to accelerate the production of reactive oxygen species (ROS), leading to oxidative stress in various organs and cells. For example, it was demonstrated that impaired glycemic control led to increased lysophosphatidylcholine

content [1], which might contribute to atherogenesis [2] and reflect oxidative modification of lipoprotein [1]. Increased oxidative stress is also thought to relate to the injury of various organs, with evidence increasingly indicating that oxidative stress may play an important role in diabetes vascular complications [3]. However, the importance of oxidative stress among diabetic patients without vascular complications is unclear.

In investigating the role of oxidative stress in diabetes, mitochondria are important organelles. A type of diabetes associated with a mutation of mitochondrial DNA has been identified [4]. Mitochondria, which provide energy for adenosine triphosphate through oxidative phosphorylation by the electron transport chain, are also the principal source of ROS resulting from imperfect electron transport. Therefore, many extensive *in vitro* investigations have been carried out about the relationship between oxidative stress and diabetes. However, few clinical indicators exist, because of the difficulty of assessing oxidative stress levels from mitochondria.

Mononuclear cells such as lymphocytes and monocytes are principally inflammatory cells. Once activated, they produce ROS and play an important role not only in the immune response but also in the first stages of atherosclerotic development [5,6]. An increase in oxidative stress is thought to promote atherogenesis [7], and diabetes mellitus is considered to be one of the major risk factors for myocardial infarction [8]. Accordingly, the possibility exists that a functional disorder of the mononuclear cells might affect the production of the cells' oxidative stress because of a hyperglycemic state due to diabetes.

Therefore, we obtained living mononuclear cells from both healthy subjects and diabetic subjects without clinical vascular complications and stained them with dihydrorhodamine-123 (DHR-123), which selectively accumulates in the mitochondria [9]. We subsequently measured the mitochondrial oxidative stress levels of the cells directly before and after addition of phorbol 12-myristate 13-acetate (PMA), which is a protein kinase C (PKC) activator that generates oxidative stress. Comparing these data from the healthy and diabetic subjects, we evaluated the mitochondrial oxidative stress levels of mononuclear cells in diabetes before the development of clinical vascular complications. We also investigated the relationship between these levels and both urinary 8-hydroxydeoxyguanosine (8OHdG) [10] and 8-epi-prostaglandin F2α (isoprostane) [11], which are thought to be putative biomarkers of total systemic oxidative stress *in vivo*.

Materials And Methods

The study group consisted of 52 age-matched apparently healthy volunteers (25 men and 27 women) and 26 subjects with type 2 diabetes (16 men and 10 women, mean duration of diabetes: 8.5 ± 0.5 years), who had consulted an outpatient clinic of diabetes and been diagnosed free from diabetic microangiopathy. All subjects were nonsmokers, free from pain or inflammatory diseases, known myocardial infarction, stroke or arteriosclerosis obliterans, and were aged between 45 and 80 (mean: 62.2 ± 1.0) years. Diabetic subjects and healthy volunteers were treated if they had dyslipidemia (8 and 4 subjects, respectively) or hypertension (11 and 9 subjects, respectively). Eight diabetic subjects were treated by diet and exercise for glycemic control, and 18 subjects by oral hypoglycemic agents. A definition of diabetes was based on the 1998 World Health Organization (WHO) criteria [12]. All diabetic patients were consulted and were classified for diabetic retinopathy by trained ophthalmologists. Nephropathy was defined as the presence of microalbuminuria or proteinuria, and neuropathy was diagnosed if subjective symptoms or a decline in tendon reflexes was present. All subjects provided blood and spot urine samples after an overnight fast for biochemical, hematological parameters and mononuclear cell isolation. We used an automated enzymatic procedure to determine serum triglycerides, total cholesterol, HDL-cholesterol and LDL-cholesterol level. The concentration of blood glucose was determined with the hexokinase-glucose-6-phosphate dehydrogenase method. HbA_{1c} was measured using ion-exchange high-performance liquid chromatography. Blood pressure (mmHg) was measured by a standard mercury sphygmomanometer with the subjects in the sitting position; standing height (cm) and body weight (kg) were also measured. All subjects were informed about the objectives and methods of this study and written informed consent was obtained from them.

Mononuclear cell isolation was carried out by heparinized blood samples using Cappel lymphocyte separation medium (ICN Biomedicals, Costa Mesa, CA), according to the method previously described [13]. Oxidative stress was analyzed using DHR-123 (Molecular Probe, Eugene, OR) by the previously described procedure [14]. In brief, DHR-123 that accumulates in the mitochondria is a nonfluorescent compound, but when converted to rhodamine-123 by the action of oxidative stress in the mitochondria, it becomes highly fluorescent. This enabled us to directly monitor the mitochondrial oxidative stress levels. The cells were washed twice, counted and resuspended to 1×10^6 cells/mL in RPMI 1640 with 1% bovine serum. They were divided into three tubes. One was expressed for the control without the fluorescent compound (Control: C), one was for baseline mitochondrial oxidative stress levels with DHR-123 (1 μM) (Basal: B), and the last was for stimulated mitochondrial oxidative stress levels with both DHR-123 (1 μM) and PMA (50 nM) (Sigma-Aldrich, St. Louis, MO) (PMA-stimulated: S). The fluorescent levels of tube B were considered to be a reflection of baseline mitochondrial oxidative stress because rhodamine-123 became fluorescent from mitochondrial oxidative stress that already existed at ordinary status without PKC activation. The fluorescent levels of tube S were assumed to be a reflection of the stimulated status of mitochondrial oxidative stress due to respiratory burst with PKC activation. The cells in the three tubes were incubated at 37 °C for 90 min. They were then washed

once rapidly and resuspended in 400 μl of RPMI 1640 with 1% bovine serum and stored on ice until flow cytometry was carried out.

Flow cytometry was performed on a FACScan (Becton Dickinson, Mountain View, CA) and analyzed at a level of 10 000 events for each test. The oxidative stress levels of mononuclear cells were measured using a fluorescence histogram through gated flow cytometry of viable cells. The degree of fluorescence was expressed by the mean fluorescence intensity (MFI) calculated for each tube by CELL Quest ver.3.2.1. The relative fluorescence variation (RFV), which is the rate of increase between oxidative stress levels before PMA stimulation, that is, MFI(B)−MFI(C), and after PMA stimulation, that is, MFI(S)−MFI(C), was calculated with minor modifications according to the previously described procedure [15]. Ultimately, it was calculated by the following formula: [(MFI(S)−MFI(C))−(MFI(B)−MFI(C))/(MFI(B)−MFI(C))], namely, (MFI(S)−MFI(B)/MFI(B)−MFI(C)). We also measured both urinary 8OHdG and isoprostane, which could be used to estimate the sum of systemic oxidative stress levels without invasive examinations. Urinary 8OHdG was measured by ELISA kit (NOF Corporation, Tokyo, Japan), as described previously [11,16]. Urinary isoprostane was measured by EIA kit (Oxford Biomedical Research, Inc., Oxford, MI) [17]. These results were expressed as the ratios to the urinary creatinine measured in the same urine samples.

Results were indicated as mean ± SE. The degree of obesity was expressed by the body mass index (BMI) (kg/m^2), calculated as body weight divided by the square of height. Parametric comparisons between healthy and diabetic subjects were performed by analysis of covariance (ANCOVA) with sex as a covariate. In this analysis, because triglycerides, BMI, urinary 8OhdG and isoprostane did not show normal distributions, these data were analyzed after logarithmic transformation. Also, regression analyses were performed by two sets to investigate associations between RFV, as a dependent variable, and each factor, as an independent variable: the first set, adjusted for age and sex (1 = men, 0 = women), and the second set, adjusted for age, sex and diabetes (1 = diabetes, 0 = not diabetes). For all data analysis, SAS package version 8.2 (SAS Institute, Cary, NC) was used.

Results

Clinical characteristics of the study subjects are shown in Table 1. Compared to healthy subjects, diabetic subjects had higher systolic blood pressure, although the difference was not significant ($P = 0.083$). BMI, total cholesterol, HDL-cholesterol and LDL-cholesterol, which were thought to be indicators for the risk of cardiovascular disease, were not significantly different between the two groups. However, diabetic subjects had significantly higher fasting glucose and HbA_{1c} levels ($P < 0.0001$). Thus, these results indicated that the clinical characteristics of these groups did not differ significantly, except in the case of glucose metabolism.

Table 1. Clinical characteristics of the study subjects adjusted for sex

	Healthy subjects	Diabetics	P
Numbers of subjects (men/women)	25/27	16/10	
Age (years)	62.4 ± 1.2	62.1 ± 1.7	0.907
Body mass index (kg/m^2)	24.0 ± 0.4	24.9 ± 0.6	0.213
Systolic blood pressure (mmHg)	129 ± 2	135 ± 3	0.083
Diastolic blood pressure (mmHg)	78 ± 1	82 ± 2	0.161
Total cholesterol (mmol/l)	5.28 ± 0.10	5.09 ± 0.14	0.275
Triglycerides (mmol/l)	1.50 ± 0.16	1.96 ± 0.23	0.176
HDL-cholesterol (mmol/l)	1.43 ± 0.05	1.49 ± 0.07	0.475
LDL-cholesterol (mmol/l)	3.09 ± 0.09	2.85 ± 0.13	0.140
HbA_{1c} (%)	5.2 ± 0.1	7.1 ± 0.1	<0.0001
Fasting glucose (mmol/l)	5.5 ± 0.3	9.5 ± 0.5	<0.0001

Data are expressed as means ± SE.

Each degree of oxidative stress level by calculation of this fluorescence and the data of urinary oxidative stress markers are shown in Table 2. The baseline oxidative stress levels without PMA were higher among diabetic subjects than healthy subjects, but not significantly ($P = 0.549$). On the other hand, diabetic subjects had significantly higher oxidative stress levels stimulated by PMA and RFV ($P < 0.0001$ for each). Urinary 8OHdG and isoprostane were also significantly higher among diabetic subjects ($P = 0.019$, $P = 0.009$ respectively).

Next, regression analyses were performed to determine the relationships between RFV and each parameter (Table 3). In the first set, adjusted for age and sex, RFV was significantly associated with urinary 8OHdG and isoprostane ($P = 0.039$, $P = 0.017$ respectively). In the second set, adjusted for age, sex and diabetes, it was not statistically significant, but had a suggestive association with urinary 8OHdG and isoprostane ($P = 0.081$, $P = 0.091$ respectively).

Discussion

In this study, mitochondrial oxidative stress levels of mononuclear cells from peripheral blood were not

Table 2. Comparisons of basal and PMA-stimulated oxidation levels or the urinary oxidation markers between healthy subjects and diabetic subjects adjusted for sex

	Healthy subjects	Diabetics	P
Control (C) (MFI)	8.7 ± 0.8	10.6 ± 1.1	0.152
Basal (B) (MFI)	281.4 ± 18.8	301.1 ± 26.8	0.549
PMA-stimulated (S) (MFI)	437.4 ± 92.4	1218.0 ± 131.7	<0.0001
RFV	0.70 ± 0.42	4.02 ± 0.60	<0.0001
Urinary 8OHdG (ng/mg · creatinine)	8.8 ± 0.5	11.1 ± 0.8	0.019
Urinary isoprostane (ng/g · creatinine)	0.32 ± 0.13	0.87 ± 0.18	0.009

Data are expressed as means ± SE. PMA, phorbol 12-myristate 13-acetate; MFI, mean fluorescence intensity; RFV, the relative fluorescence variation.

Table 3. Regression analyses between RFV and each parameter

	Adjusted for age and sex		Adjusted for age, sex and diabetes	
	β	P	β	P
Body mass index (kg/m^2)	−0.015	0.914	−0.096	0.432
SBP (mmHg)	−0.020	0.473	−0.037	0.144
DBP (mmHg)	−0.036	0.337	−0.047	0.163
Total cholesterol (mmol/L)	0.422	0.450	0.735	0.141
Triglycerides (mmol/L)	0.154	0.651	−0.105	0.735
HDL-cholesterol (mmol/L)	1.362	0.220	1.001	0.314
LDL-cholesterol (mmol/L)	−0.005	0.993	0.427	0.427
Urinary 8OHdG (ng/mg · creatinine)	0.202	0.039	0.152	0.081
Urinary isoprostane (ng/g · creatinine)	0.092	0.017	0.062	0.091

RFV, the relative fluorescence variation.

significantly higher at baseline, but when stimulated by PKC, oxidative stress levels were significantly higher in diabetic subjects without clinical vascular complications than in healthy subjects. Additionally, it was suggested that whole oxidative stress levels tended to increase in diabetic subjects, because urinary 8OHdG and isoprostane levels were significantly higher, and oxidative stress generation was increased and/or the scavenging mechanisms against oxidative stress under PKC stimulation were diminished in diabetic subjects even before the development of clinical vascular complications.

We should consider that these results have two possible explanations. The first possibility is that diabetes might induce oxidative stress. The second is that, conversely, oxidative stress might induce diabetes. Concerning the first possibility, some activation pathways of oxidative stress in diabetes are theorized: hyperactivity of polyol pathway [18]; increased formation of advanced glycation end products [19] and glucose-induced activation of PKC [20]. PKC is a phospholipid-dependent serine/threonine protein kinase, activated by diacylglycerol that is mainly derived from the *de novo* pathway from the glycolytic intermediates [21,22]. Thus, a hyperglycemic state stimulates ROS production through PKC activation [20]. In addition, it was reported recently that PKC was activated by hyperglycemia-induced oxidative phosphorylation in cultured bovine aortic endothelial cells [23]. However, even in diabetic patients, we did not detect a significant increase in mitochondrial oxidative stress levels at baseline that was supposed to be generated by PKC activation, but we detected an increase in the level upon stimulation by the additive PKC activator (Table 2). Accordingly, it was suggested that PKC was not always activated in diabetic subjects without clinical vascular complications, and that the generation mechanisms of the mitochondrial oxidative stress were accelerated and/or scavenging mechanisms against it were decreased under PKC activation compared to healthy subjects. Actually, a hyperglycemic state is reported to impair radical scavenging activity [24].

We cannot deny the second possibility that oxidative stress itself is related to the development and progression of diabetes; that is, some individuals might be susceptible to the development and progression of diabetes as a result of impairment of sufficient oxidative stress level control, when PKC was activated in various degrees by their own genetic makeup or environmental factors. As a result, diabetic subjects might be at high oxidative stress levels. The possibility exists that oxidative stress of mononuclear cells circulating throughout the body might injure pancreatic β cells, leading to impaired glucose metabolism. In addition, increased oxidative stress could precede the development of endothelial dysfunction and insulin resistance [25]. The imbalance between the generation and scavenging mechanisms of oxidative stress might be associated with the pathophysiology of diabetes. Overproduction of the mitochondrial ROS might induce cell injury, hypothetically leading to a weak but chronic inflammatory state, which is presently believed to relate to the development of diabetes. For example, lysophosphatidylcholine, known to be a major phospholipid compartment of oxidized LDL, was thought to contribute to acute and chronic inflammation [2], and high levels of C-reactive protein, a marker of inflammation, were reported to be one of the risk factors for development of diabetes [26,27]. Thus, there is a possibility that both oxidative stress and its resultant chronic inflammation might be involved in some of the mechanisms of diabetes development.

Because we found in this study that mitochondrial oxidative stress was related to diabetes, a sensitive marker that is suitable for monitoring oxidative stress is anticipated. In general, diabetic patients have high oxidative stress levels for various reasons, for instance, because of obesity [28], NADPH oxidase activation in monocyte [29] and so forth. Urinary 8OHdG [10] and isoprostane [11] are noteworthy markers; they were significantly higher among diabetic subjects than healthy subjects in this study (Table 2). However, they are thought to be a reflection of the sum of systemic oxidative stress levels rather than a reflection of the metabolites of oxidative stress from a specific organ. To the contrary, RFV was thought to be a marker reflecting the mitochondrial oxidative stress levels more directly. In our study, although it had a significant relationship to both urinary 8OHdG and isoprostane adjusted for age and sex, these relationships disappeared after adjustment for age, sex and diabetes (Table 3). Thus, it was suggested that mitochondrial oxidative stress, as well as each urinary oxidative stress marker, might be strongly affected by glucose metabolism.

This study has some limitations. First, it remains a possibility that type 2 diabetes subjects might be inadvertently included in healthy subjects even when they undergo the 75- g oral glucose tolerance test. However, diabetes in this study was diagnosed according to WHO criteria [12], and all healthy subjects were confirmed to have a fasting glucose level less than 7.0 mmol/L and, in addition, an HbA_{1c} level less than 6.5%. Second, the results of this study

might be modified by the diabetes medication. For example, one patient was treated for diabetes by pioglitazone, one of the thiazolidine derivatives, and six patients were treated for hypertension by angiotensin II receptor blockers. These drugs have reported to reduce ROS generation [30–32]. However, the results of our data such as RFV and urinary markers did not differ significantly according to either these drugs or the oral hypoglycemic agents (data not shown), but the problem remains whether the improvement of glycemic control improves the balance of mitochondrial oxidative stress. Third, DHR-123 used to measure oxidative stress is accumulated in mitochondria according to the Nernst equation, due to their high membrane potential [9]. Consequently, the possibility remains that the changes in the mitochondrial membrane potential, not the changes in the mitochondrial oxidative stress level, might alter the uptake of this dye and hence alter the fluorescence measured and the degree of oxidative stress inferred. We must consider that, at least in part, changes in mitochondrial membrane potential could account for the differences in the fluorescence observed following PMA stimulation.

In summary, the mitochondrial oxidative stress levels of mononuclear cells from peripheral blood at baseline among diabetic subjects without clinical vascular complications were not statistically higher than those among healthy subjects, but were significantly higher under PMA stimulation. This result indicated an imbalance of generation and elimination of mitochondrial oxidative stress among diabetic subjects before the development of clinical vascular complications.

Acknowledgements

We are grateful to Mr Shinsuke Matsuura and the entire staff at the Radiation Effects Research Foundation in Hiroshima for their outstanding assistance, and to Dr Masamichi Okubo for his valuable suggestions.

References

1. Takahara N, Kashiwagi A, Nishio Y, *et al.* Oxidized lipoproteins found in patients with NIDDM stimulated radical-induced monocyte chemoattractant protein-1 mRNA expression in cultured human endothelial cells. *Diabetologia* 1997; **40**: 662–670.
2. Kume N, Cybulsky MI, Gimbrone MA Jr. Lysophosphatidylcholine, a component of atherogenic lipoproteins, induces mononuclear leukocyte adhesion molecules in cultured human and rabbit arterial endothelial cells. *J Clin Invest* 1992; **90**: 1138–1144.
3. Giugliano D, Paolisso G, Ceriello A. Oxidative stress and diabetic vascular complications. *Diabetes Care* 1996; **19**: 257–267.
4. Kadowaki T, Kadowaki H, Mori Y, *et al.* A subtype of diabetes mellitus associated with a mutation of mitochondrial DNA. *N Engl J Med* 1994; **330**: 962–968.
5. Ross R. Atherosclerosis is an inflammatory disease. *Am Heart J* 1999; **138**: S419–S420.
6. Hansson GK. Regulation of immune mechanisms in atherosclerosis. *Ann N Y Acad Sci* 2001; **947**: 157–165.
7. Stamler J, Vaccaro O, Neaton JD, Wentworth D. Diabetes, other risk factors, and 12-yr cardiovascular mortality for men screened in the multiple risk factor intervention trial. *Diabetes Care* 1993; **16**: 434–444.
8. Haffner SM, Lehto S, Rönnemaa T, Pyörälä K, Laakso M. Mortality from coronary heart disease in subjects with type 2 diabetes and in nondiabetic subjects with and without prior myocardial infarction. *N Engl J Med* 1998; **339**: 229–234.
9. Johnson LV, Walsh ML, Chen LB. Localization of mitochondria in living cells with rhodamine 123. *Proc Natl Acad Sci USA* 1980; **77**: 990–994.
10. Leinonen J, Lehtimaki T, Toyokuni S, *et al.* New biomarker evidence of oxidative DNA damage in patients with non-insulin-dependent diabetes mellitus. *FEBS Lett* 1997; **417**: 150–152.
11. Davì G, Ciabattoni G, Consoli A, *et al.* In vivo formation of 8-iso-prostaglandin F2α and platelet activation in diabetes mellitus: effects of improved metabolic control and vitamin E supplementation. *Circulation* 1999; **99**: 224–229.
12. Alberti KGMM, Zimmet PZ. Definition, diagnosis and classification of diabetes mellitus and its complications. Part 1: diagnosis and classification of diabetes mellitus provisional report of a WHO consultation. *Diabet Med* 1998; **15**: 539–553.
13. Orie NN, Zidek W, Tepel M. Reactive oxygen species in essential hypertension and non-insulin-dependent diabetes mellitus. *Am J Hypertens* 1999; **12**: 1169–1174.
14. Clutton SM, Townsend KMS, Walker C, Ansell JD, Wright EG. Radiation-induced genomic instability and persisting oxidative stress in primary bone marrow cultures. *Carcinogenesis* 1996; **17**: 1633–1639.
15. Ostrovidov S, Franck P, Joseph D, *et al.* Screening of new antioxidant molecules using flow cytometry. *J Med Chem* 2000; **43**: 1762–1769.
16. Shimosawa T, Shibagaki Y, Ishibashi K, *et al.* Adrenomedullin, an endogeneous peptide, counteracts cardiovascular damage. *Circulation* 2002; **105**: 106–111.
17. Roberts CK, Vaziri ND, Barnard RJ. Effect of diet and exercise intervention on blood pressure, insulin, oxidative stress, and nitric oxide availability. *Circulation* 2002; **106**: 2530–2532.
18. Barnett PA, Gonzalez RG, Chylack LT Jr, Cheng HM. The effect of oxidation on sorbitol pathway kinetics. *Diabetes* 1986; **35**: 426–432.
19. Mullarkey CJ, Edelstein D, Brownlee M. Free radical generation by early glycation products: a mechanism for accelerated atherogenesis in diabetes. *Biochem Biophys Res Commun* 1990; **31**: 932–939.
20. Inoguchi T, Li P, Umeda F, *et al.* High glucose level and free fatty acid stimulate reactive oxygen species production through protein kinase C-dependent activation of NAD(P)H oxidase in cultured vascular cells. *Diabetes* 2000; **49**: 1939–1945.
21. Inoguchi T, Xia P, Kunisaki M, Higashi S, Feener EP, King GL. Insulin's effect on protein kinase C and diacylglycerol induced by diabetes and glucose in vascular tissues. *Am J Physiol* 1994; **267**: E369–E379.
22. Craven PA, Davidson CM, DeRubertis FR. Increase in diacylglycerol mass in isolated glomeruli by glucose from de novo synthesis of glycerolipids. *Diabetes* 1990; **39**: 667–674.
23. Nishikawa T, Edelstein D, Du XL, *et al.* Normalizing mitochondrial superoxide production blocks three pathways of hyperglycemic damage. *Nature* 2000; **404**: 787–790.
24. Kashiwagi A, Asahina T, Ikebuchi M, *et al.* Abnormal glutathione metabolism and increased cytotoxicity caused by H_2O_2 in human umbilical vein endothelial cells cultured in high glucose medium. *Diabetologia* 1994; **37**: 264–269.
25. Gopaul NK, Manraj MD, Hebe A, *et al.* Oxidative stress could precede endothelial dysfunction and insulin resistance in Indian Mauritians with impaired glucose metabolism. *Diabetologia* 2001; **44**: 706–712.
26. Pradhan A, Manson JE, Rifai N, Buring JE, Ridker PM. C-reactive protein, interleukin 6, and risk of developing type 2 diabetes mellitus. *JAMA* 2001; **286**: 327–334.
27. Barzilay JI, Abraham L, Heckbert SR, *et al.* The relation of markers of inflammation to the development of glucose disorders in the elderly: the cardiovascular health study. *Diabetes* 2001; **50**: 2384–2389.
28. Dandona P, Mohanty P, Ghanim H, *et al.* The suppressive effect of dietary restriction and weight loss in the obese on the generation of reactive oxygen species by leukocytes, lipid peroxidation, and protein carbonylation. *J Clin Endocrinol Metab* 2001; **86**: 355–362.

29. Dandona P, Thusu K, Cook S, *et al.* Oxidative damage to DNA in diabetes mellitus. *Lancet* 1996; 347: 444–445.
30. Garg R, Kumbkarni Y, Aljada A, *et al.* Troglitazone reduces reactive oxygen species generation by leukocytes and lipid peroxidation and improves flow-mediated vasodilatation in obese subjects. *Hypertension* 2000; 36: 430–435.
31. Dandona P, Aljada A. A rational approach to pathogenesis and treatment of type 2 diabetes mellitus, insulin resistance, inflammation, and atherosclerosis. *Am J Cardiol* 2002; 90: 27G–33G.
32. Dandona P, Kumar V, Aljada A, *et al.* Angiotensin II receptor blocker valsartan suppresses reactive oxygen species generation in leukocytes, nuclear factor-kappa B, in mononuclear cells of normal subjects: evidence of an anti-inflammatory action. *J Clin Endocrinol Metab* 2003; 88: 4496–4501.

Expression Characteristics and Stimulatory Functions of CD43 in Human CD4$^+$ Memory T Cells: Analysis Using a Monoclonal Antibody to CD43 That Has a Novel Lineage Specificity[1]

Seishi Kyoizumi,[2]* Takaaki Ohara,† Yoichiro Kusunoki,* Tomonori Hayashi,* Kazuaki Koyama,* and Naohiro Tsuyama‡

We have used HSCA-2, an mAb that recognizes a sialic acid-dependent epitope on the low molecular mass (~115-kDa) glycoform of CD43 that is expressed in resting T and NK cells, to examine the expression characteristics and stimulatory functions of CD43 in human CD4$^+$ memory T cells. Having previously reported that the memory cells that respond to recall Ags in a CD4$^+$CD45RO$^+$ T cell population almost all belong to a subset whose surface CD43 expression levels are elevated, we now find that exposing these same memory T cells to HSCA-2 mAb markedly increases their proliferative responsiveness to recall Ags. We think it unlikely that this increase in responsiveness is a result of CD43-mediated monocyte activation, especially given that the HSCA-2 mAb differs from all previously used CD43 mAbs in having no obvious binding specificity for monocyte CD43. Predictably, treatment with HSCA-2 mAb did not lead to significant recall responses in CD4$^+$CD45RO$^+$ T cells, whose CD43 expression levels were similar to or lower than those of naive cells. Other experiments indicated that the HSCA-2 mAb was capable of enhancing the proliferative responsiveness of CD4$^+$ memory T cells that had been exposed to polyclonal stimulation by monocyte-bound CD3 mAb and could also act in synergy with CD28 mAb to enhance the responsiveness of CD4$^+$ T cells to CD3 stimulation. Taken together, these findings suggest that the CD43 molecules expressed on CD4$^+$ memory T cells may be capable of enhancing the costimulatory signaling and hence providing accessory functions to TCR-mediated activation processes. *The Journal of Immunology,* **2004, 172: 7246–7253.**

CD43 (leukosialin) is a highly glycosylated transmembrane protein that is expressed in all hemopoietic cells except resting mature B cells and erythrocytes (1, 2). All CD43 molecules possess extracellular domains that consist of multiple *O*-linked carbohydrate chains (3) and show considerable m.w. heterogeneity due to differential glycosylation (4). Even within T cell populations there are at least two glycoforms of CD43 that are recognized by different mAbs. The lighter of these glycoforms has a molecular mass of 95–115 kDa, whereas that of that heavier one is between 130 and 135 kDa (5, 6). Interestingly, the heavier glycoform contains core 2 *O*-glycans, appears to be up-regulated during T cell activation (5, 7), and can be used to distinguish between memory and effector CD8$^+$ T cells in mice (8, 9). It is not yet clear exactly what CD43 does in T cells, however, especially in view of the continued existence of a number of unresolved controversies about its roles in such key processes as cell adhesion, cell death, and costimulation in TCR signaling (10).

It has, for instance, been claimed that CD43 molecules may have antiadhesive as well as proadhesive functions in T cell trafficking (9, 11–14). It has also been claimed that up-regulation of CD43 expression can have a negative effect on activation-induced cell death of T cells (15), and that Ab-mediated cross-linking of CD43 induces apoptosis of Jurkat T cells (16). CD43 also appears to play a role in T cell activation, but precisely what role remains unclear. There are, for example, Ab cross-linking experiments involving CD43 that suggest that it may have a costimulatory role in vitro (17) and act in association with the phosphorylation of signal-transducing molecules in T cell activation (18–20); other experiments using CD43-deficient mice suggest, on the contrary, that CD43 has either a negative regulatory role as a steric barrier (21) or possibly even no significant role at all (22) in T cell activation. There are several recent reports suggesting that molecular complexes between CD43 and cytoskeletal adaptor proteins are probably excluded from the immunological synapse in T cell activation in vitro (23–25) and in vivo (26). Some of these reports include suggestions that this relocalization of CD43 is necessary for activation-induced cytokine production (23, 27), although there is at least one recent study that comes to precisely the opposite conclusion (28). The functional significance of redistribution of CD43 in T cell activation is therefore very unclear. Nevertheless, given that CD43 expression levels appear to be considerably elevated in memory T cell populations in humans (29–31) and mice (15), it seems reasonable to assume that CD43 has an important part to play in one or more aspects of the memory T cell responses.

*Laboratory of Immunology, Department of Radiobiology/Molecular Epidemiology, Radiation Effects Research Foundation, Hiroshima, Japan; †Life Science Laboratories, Life Science RD Center, Kaneka Corp., Takasago, Japan; and ‡Cellular Signal Analysis, Department of Bio-Signal Analysis, Applied Medical Engineering Science, Yamaguchi University Graduate School of Medicine, Ube City, Japan

Received for publication November 11, 2003. Accepted for publication April 2, 2004.

The costs of publication of this article were defrayed in part by the payment of page charges. This article must therefore be hereby marked *advertisement* in accordance with 18 U.S.C. Section 1734 solely to indicate this fact.

[1] This publication is based on research performed at the Radiation Effects Research Foundation (RERF), Hiroshima and Nagasaki, Japan. RERF is a private nonprofit foundation funded equally by the Japanese Ministry of Health, Labor, and Welfare (MHLW) and the U.S. Department of Energy, the latter through the National Academy of Sciences. This work was supported by RERF Research Protocols 1-93 and 4-02 and in part by funds for Research Promotion on AIDS Control from MHLW.

[2] Address correspondence and reprint requests to Dr. Seishi Kyoizumi, Laboratory of Immunology, Department of Radiobiology/Molecular Epidemiology, Radiation Effects Research Foundation, 5-2 Hijiyama Park, Minami Ward, Hiroshima 732-0815, Japan. E-mail address: kyoizumi@rerf.or.jp

0022-1767/04/$02.00

We have recently described how HSCA-2, a novel CD43 mAb, can be used for the classification of human $CD4^+CD45RO^+$ memory T cells into three subsets on the basis of differences in their CD43 expression (31). In this classification, cells of the first of the three subsets (the M1 subset) express elevated levels of CD43, whereas cells of the M2 subset express CD43 levels similar to those of naive cells, and cells of the M3 subset express reduced CD43 levels. We also found that the M1 subset contains the highest proportion of recall Ag-reactive precursors and secretes substantially more IFN-γ and IL-4. The majority of effector memory T cells ($CCR7^-$) (32) are assumed to belong to this subset (31). However, as ~70% of the cells in the M1 subset express CCR7, the subset may also contain central memory T cells. The M2 subset cells are less mature memory cells that retain longer telomeres than do cells of the M1 and M3 subsets, and their memory functionality (including recall Ag reactivity) appears to be marginal (31). The M3 subset consists of cells that are anergic to TCR-mediated stimuli and prone to apoptosis (31). As the level of CD43 expression is correlated with recall Ag reactivity, it is possible that CD43 molecules will prove to have some accessory role in the activation of human $CD4^+$ memory T cells.

In this paper we describe immunological properties and expression characteristics of the CD43 molecules that are recognized by HSCA-2 mAb. We go on to examine the functional properties of these molecules in the proliferative responses of $CD4^+$ memory T cells. The results described in this report demonstrate that the HSCA-2 mAb specifically recognizes a neuraminidase-sensitive epitope of a low molecular mass glycoform (115 kDa) of CD43 that is predominantly expressed in lymphoid populations. It is also suggested that the CD43 glycoform recognized by HSCA-2 mAbs could play an accessory part in the recall Ag-specific responses of mature $CD4^+$ memory T cells (i.e., M1 subset cells). HSCA-2 mAb has therefore proven to be a useful molecular probe for both the classification and the functional analysis of human $CD4^+$ memory T cells. The implications of our work for the involvement of CD43-mediated stimulatory signaling in the activation of $CD4^+$ T cells are discussed.

Materials and Methods

Production of HSCA-2 mAb

The HSCA-2 hybridoma is a product of the fusion of NS1 mouse myeloma cells with splenocytes from BALB/c mice immunized by injection of human KG-1 cells (31). Immunization, fusion, selection, and cloning protocols were essentially as described previously (33). Hybridoma supernatants were initially screened for reactivity with KG-1 cells by indirect immunofluorescence. The HSCA-2 hybridoma was selected for further study because of its unique specificity of reactivity with PBMC and cord blood $CD34^+$ stem cells. Isotype characterization showed that the HSCA-2 mAb was of the IgG1 subclass. Ascites fluid was obtained from SCID mice injected with the HSCA-2 hybridoma. After purification from ascites fluid by DE52 ion exchange chromatography, HSCA-2 mAb was labeled with FITC (Sigma-Aldrich, St. Louis, MO) for flow cytometry. Fab of HSCA-2 mAb were prepared by digestion with papain (34). This mAb was filed for participation in the Eighth International Workshop and Conference on Human Leukocyte Differentiation Ags (to be held in Adelaide, Australia).

Other mAbs

Unconjugated CD28 mAb (clone CD28.2) (35), used for T cell culture, was purchased from Coulter-Immunotech (Marseilles, France). Unconjugated and FITC-conjugated CD43 mAbs, DFT-1 (1), L10 (36), and 1G10 (37), were obtained from Coulter-Immunotech, Caltag Laboratories (Burlingame, CA), and BD PharMingen (San Diego, CA), respectively. PE-labeled CD4, CD8, CD14, CD19, and CD56 mAbs and PerCP-labeled CD4 and CD8 mAbs were purchased from BD Biosciences (San Jose, CA). PE-labeled CD45RO mAb was obtained from Caltag Laboratories.

Transfection of CD43 cDNA

Total RNA of KG-1 cells was isolated with TRIzol reagent (Invitrogen, Carlsbad, CA). First-strand cDNA primed with oligo$(dT)_{30}$ was synthesized using SuperScript II reverse transcriptase (Invitrogen). CD43 cDNA was PCR-amplified with the primers 5′-ctcttgctcctgcctgtttgc-3′ and 5′-catggtggtgggtgcctgtaa-3′ using Advantage cDNA polymerase mix (Clontech Laboratories, Palo Alto, CA) and cloned into pCR2.1 TA cloning vector (Invitrogen). The sequence-verified clone was recloned into the *Eco*RI site of pIRESneo (Clontech Laboratories) and designated pIRESneo hCD43. Subsequently, 30 μg of pIRESneo hCD43 or pIRESneo (negative control) was electroporated into 2×10^6 HeLa cells in 200 μl of PBS by GenePulser (Bio-Rad, Hercules, CA) at 0.7 kV and 25 μF. Cells were treated with 1 mg/ml G418 for 2 wk. Drug-resistant colonies were selected and expanded to confirm CD43 expression by flow cytometry. HeLa transfectant cells expressing high levels of CD43 were isolated by a cell sorter for additional experiments.

Cell preparations and flow cytometry

For direct immunofluorescence of cultured cell lines, 2×10^5 CD43- or mock-transfected HeLa and KG-1 cells were stained with 1 μg of FITC-labeled HSCA-2, DFT-1, and MOPC21 mAbs for 45 min on ice. For the analyses of CD43 glycoepitopes, 2×10^6 KG-1 cells were treated with neuraminidase (0.1 U/ml in PBS) for 30 min at 37°C. For competitive inhibition, KG-1 cells were pretreated with various amounts of HSCA-2 or DFT-1 mAbs (12.5–200 μg/ml) for 1 h on ice and then stained with FITC-labeled HSCA-2 and DFT-1 mAbs for 45 min. FACScan (BD Biosciences) was used for flow cytometric analyses.

For flow cytometry of human blood cells, PBMCs from healthy adult volunteers ($n = 6$) and cord blood mononuclear cells ($n = 3$) were isolated by density centrifugation in Ficoll-Hypaque (density, 1.077 g/ml; ICN Biomedical, Aurora, OH). Granulocytes were isolated by double-layered density centrifugation in Ficoll-Hypaque (density, 1.077 and 1.119 g/ml; Wako Pure Chemical, Osaka, Japan) according to the manufacturer's instructions. For isolation of monocytes, $CD14^+$ cells were purified from PBMCs by positive enrichment using autoMACS (Miltenyi Biotec, Bergish Gladbach, Germany) according to the manufacturer's instructions. Enriched monocytes also were used for immunoprecipitation and proliferation assay, as described below.

For single-color analysis of purified monocytes and granulocytes, cells were stained with FITC-labeled CD43 mAbs and analyzed by flow cytometry with a gate in a region for monocytes or granulocyte fractions on the forward and side light scatter profiles. For two-color analysis of lymphocytes, PBMCs were stained with PE-labeled CD4, CD8, CD19, and CD56 in combination with FITC-labeled CD43 mAbs. Cord blood mononuclear cells were stained with FITC-labeled CD43 and PE-labeled CD34 mAbs. For triple-color analysis, PBMCs were stained with FITC-labeled CD43, PE-conjugated CD45RO, and PerCP-labeled CD4 mAbs. $CD4^+$ lymphocytes were gated on forward/side scatter and PerCP fluorescence. The proportions of $CD4^+$ $CD45RO^-$ cells (RO^- subset) and $CD4^+$ $CD45RO^+$ cells expressing high (M1 subset), intermediate (M2), and low (M3) levels of CD43 were measured by flow cytometry with FACScan (see Fig. 4).

For preparation of activated $CD4^+$ T cells, MACS-purified $CD4^+$ T cells were stimulated with immobilized anti-CD3 mAb (OKT-3) in the presence of IL-2 (10 ng/ml) for 4 days in RPMI 1640 supplemented with 10% FCS. Immobilized CD3 mAb was prepared by binding OKT3 mAb (10 μg/ml in sodium bicarbonate buffer, pH 9.6) in 24-well plates at room temperature for 2 h, then washing the plates with RPMI 1640 supplemented with 10% FCS.

For isolation of the four $CD4^+$ T cell subsets, M1, M2, M3, and $CD45RO^-$, $CD4^+$ cells were purified by negative enrichment using MACS as described previously (31). MACS-purified $CD4^+$ T cells were stained with FITC-labeled HSCA-2 and PE-labeled CD45RO mAbs. After incubation with propidium iodine at 10 μg/ml for 15 min to gate out dead cells, $CD4^+$ T cells in the four subsets were sorted by a single laser cell sorter (FACStar; BD Biosciences). During cell sorting, stained and sorted cell suspensions were maintained at 4°C by a cooling circulation system.

Cell proliferation assay

For proliferative response to recall Ags, PBMCs (5×10^4 cells/well) in 96-well, flat-bottom plastic plates were stimulated with tuberculosis purified protein derivative (PPD;[3] Connaught Laboratories, Ontario, Canada) or tetanus toxoid (TT; Calbiochem, La Jolla, CA) at 5 μg/ml. For total and subset $CD4^+$ T cells, T cells (5×10^4 cells/well) were stimulated with

[3] Abbreviations used in this paper: PPD, purified protein derivative; TT, tetanus toxoid.